RUNNING TITLE: OC oxidation processes across vegetation

Carbon inputs from riparian vegetation limit oxidation of physically-bound organic carbon via biochemical and thermodynamic processes

Emily B. Graham[1], Malak M. Tfaily[2], Alex R. Crump[1], Amy E. Goldman[1], Evan Arntzen[1], Elvira Romero[1], C. Tom Resch[1], David W. Kennedy[1], and James C. Stegen[1]

[1]Pacific Northwest National Laboratory, Richland, WA USA

[2]Environmental Molecular Science Laboratory, Richland, WA USA

Correspondence: Emily B. Graham, Pacific Northwest National Laboratory, PO Box 999, Richland, WA 99352, 509-372-6049, emily.graham@pnnl.gov

Keywords: terrestrial-aquatic interface, priming, recalcitrant, labile, FT-ICR-MS, aerobic metabolism

Key points.

- Riparian vegetation protects bound-OC stocks
- Biochemical and metabolic OC oxidation processes vary with vegetation
- Common thermodynamic principles underlie OC oxidation regardless of vegetation

Abstract.

In light of increasing terrestrial carbon (C) transport across aquatic boundaries, the mechanisms governing organic carbon (OC) oxidation along terrestrial-aquatic interfaces are crucial to future climate predictions. Here, we investigate biochemistry, metabolic pathways, and thermodynamics corresponding to OC oxidation in the Columbia River corridor using ultra-high resolution C characterization. We leverage natural vegetative differences to encompass variation in terrestrial C inputs. Our results suggest that decreases in terrestrial C deposition associated with diminished riparian vegetation induce oxidation of physically-bound OC. We also find that contrasting metabolic pathways oxidize OC in the presence and absence of vegetation and—in direct conflict with the 'priming' concept—that inputs of water-soluble and thermodynamically favorable terrestrial OC protects bound-OC from oxidation. In both environments, the most thermodynamically favorable compounds appear to be preferentially oxidized regardless of which OC pool microbiomes metabolize. In turn, we suggest that the extent of riparian vegetation causes sediment microbiomes to locally adapt to oxidize a particular pool of OC, but that common thermodynamic principles govern the oxidation of each pool (e.g., water-soluble or physically-bound). Finally, we propose a mechanistic conceptualization of OC oxidation along terrestrial-aquatic interfaces that can be used to model heterogeneous patterns of OC loss under changing land cover distributions.

1. Introduction

Soils and nearshore sediments comprise a C reservoir that is 3.2 times larger than the atmospheric C pool [*Burd et al.*, 2016], yet Earth System Models (ESMs) struggle to integrate mechanisms of OC oxidation into predictions of atmospheric carbon dioxide concentrations [*Todd-Brown et al.*, 2013; *Wieder et al.*, 2013; *Wieder et al.*, 2015]. In particular, OC oxidation in nearshore habitats constitutes a significant uncertainty in atmospheric C flux [*Aalto et al.*, 2003; *Battin et al.*, 2009] and knowledge on C cycling along these transitional ecosystems is necessary to accurately predict global C cycling [*Burd et al.*, 2016]. Terrestrial C inputs into aquatic systems have nearly doubled since pre-industrial times; an estimated 2.9 Pg C now crosses terrestrial-aquatic interfaces annually (vs. 0.9 Pg C yr^{-1} stored within forested ecosystems) [*Battin et al.*, 2008; *Regnier et al.*, 2013]. The magnitude of this flux has garnered significant recent attention [*Battin et al.*, 2008; *Battin et al.*, 2009; *Regnier et al.*, 2013], yet the biochemical, metabolic, and thermodynamic mechanisms governing OC oxidation along aquatic interfaces remain a crucial uncertainty in climate predictions. New molecular techniques are providing insight into OC dynamics [*Mason et al.*, 2016; *Malak M Tfaily et al.*, 2015; *M.M. Tfaily et al.*, 2017], but we still lack an understanding of why some OC remains stabilized for millennia whereas other OC is rapidly oxidized [*Schmidt et al.*, 2011].

The ability of microorganisms to oxidize complex OC is an important constraint on C cycling, as OC is a mixture of compounds with different propensities for biotic oxidation [*J Hedges and Oades*, 1997; *J I Hedges et al.*, 2000]. Within terrestrial research, OC oxidation is often framed within the concept of 'priming', whereby microbial oxidation of chemically-complex, less bioavailable OC is fueled by the addition of more bioavailable and thermodynamically favorable OC compounds [*Kuzyakov*, 2010]. However, the applicability of

45 priming in aquatic environments is unclear [*Bengtsson et al.*, 2014; *Bianchi*, 2011; *Guenet et al.*,
46 2010]. Aquatic systems, and in particular nearshore environments, frequently experience mixing
47 of terrestrial and aquatic C sources with distinct chemical character, providing a theoretical basis
48 for priming expectations [*Bengtsson et al.*, 2014; *Guenet et al.*, 2010]. Consistent with priming,
49 *Guenet et al.* [2010] have proposed that this mixing generates "hotspots" or "hot moments" of
50 biological activity facilitated by complementary C resources. Alternatively, OC stabilization in
51 sediments is tightly linked to organomineral interactions, which provide physical protection from
52 extracellular enzyme activity [*J I Hedges and Keil*, 1995; *Hunter et al.*, 2016; *Rothman and*
53 *Forney*, 2007], and the strength of these interactions may override any influence of priming.
54 Early investigations of priming effects in aquatic systems have been inconclusive, with evidence
55 both for [*Dorado-García et al.*, 2016] and against [*Bengtsson et al.*, 2014; *Catalán et al.*, 2015]
56 priming mechanisms.

57 Several new perspectives have attempted to move beyond frameworks, such as priming,
58 that depend on strict chemical definitions to predict OC oxidation [*Burd et al.*, 2016; *Cotrufo et*
59 *al.*, 2013; *Lehmann and Kleber*, 2015]. Recent work proposes that the probability of OC
60 oxidation is related to a spectrum of chemical properties and that even very complex OC can be
61 oxidized when more thermodynamically favorable OC is depleted or isolated from
62 microorganisms. For example, *Lehmann and Kleber* [2015] have proposed a 'soil continuum
63 hypothesis' whereby OC is a gradient of continuingly decomposing compounds that are variably
64 accessible for biotic oxidation, with no notion of chemically labile versus recalcitrant
65 compounds. Similarly, *Burd et al.* [2016] have suggested that OC oxidation is a 'logistical
66 problem' involving the ability of microorganisms to access and metabolize compounds. Both

concepts capture the emerging belief that chemically-complex, less thermodynamically favorable OC can be oxidized when more favorable compounds are inaccessible.

Here, we address a critical knowledge gap in predicting the global C balance [*Aalto et al.*, 2003; *Battin et al.*, 2009; *Burd et al.*, 2016; *Regnier et al.*, 2013]—mechanisms governing OC oxidation along terrestrial-aquatic interfaces. Specifically, we investigate the biochemistry, microbial metabolism, and thermodynamics of OC oxidation in nearshore water-soluble and physically-bound (i.e., mineral and microbial) OC pools along a freshwater terrestrial-aquatic interface. We leverage natural variation in riparian vegetation along the Columbia River in Eastern Washington State, the largest river in the U.S. west of the Continental Divide [*Ebel et al.*, 1989; *Moser et al.*, 2003], to examine these mechanisms in the context of spatial variation in terrestrial C deposition. Consistent with the priming paradigm, we hypothesize that (a) C deposition associated with riparian vegetation increases total aerobic metabolism and enhances oxidation of bound-OC stocks, while (b) areas without riparian vegetation foster lower rates of aerobic metabolism with minimal oxidation of bound-OC.

2. Materials and Methods

2.1. Site Description

This study was conducted along the Columbia River shoreline within the Hanford 300A (approximately 46^{o} 22’ 15.80”N, 119^{o} 16’ 31.52”W) in eastern Washington State [*Graham et al.*, 2016a; 2017; *Slater et al.*, 2010; *Zachara et al.*, 2013]. The Columbia River experiences shoreline geographic variation in vegetation patterns, substrate geochemistry, and microbiome composition [*Arntzen et al.*, 2006; *Lin et al.*, 2012; *Peterson and Connelly*, 2004; *Slater et al.*, 2010; *James C Stegen et al.*, 2016; *James C. Stegen et al.*, 2012; *Zachara et al.*, 2013].

Accordingly, the Hanford Reach of the Columbia River embodies an ideal natural system in which to examine heterogeneity of terrestrial OC inputs and subsequent OC oxidation mechanisms.

Liquid N_2-frozen sediment profiles (0-60 cm) were collected at two transects within shoreline stretches with or without riparian vegetation (hereafter, V and NV for 'vegetated' and 'not vegetated', Table 1) perpendicular to the Columbia River in March 2015, separated by a distance of ~170m. V was characterized by a moderately sloping scour zone, small boulders; and vegetation consisted of woody perennials *Morus rubra* (Red Mulberry) and *Ulmus rubra* (Slippery Elm), with a closed canopy. Upper bank samples were collected within the root zone. In contrast, NV was characterized by a gradually sloping scour zone and cobbled armor layer. We collected profiles at three locations in each transect with 5m spacing within a spatial domain of ~175 x 10m. In each transect, the lower bank profile was located at ~0.5m (vertical distance) below the water line and the upper bank profile was located ~0.5m (vertical distance) above the water line approximately 10m horizontal distance, with the third profile situated at the midpoint. Each profile was sectioned into 10-cm intervals from 0-60cm, and OC composition (see below for Methods) did not differ across upper (0-10cm) to lower (50-60cm) sections in each profile. To provide sufficient sample size (n >15 at each transect) for cross-site comparisons, each 10-cm section was used as a replicate sample.

2.2. Sample Collection

Liquid N_2-frozen sediment profiles were collected as outlined in *Moser et al.* [2003] using a method developed by *Lotspeich and Reed* [1980] and modified by *Rood and Church* [1994]. A pointed stainless steel tube (152 cm length, 3.3 cm outside diameter, 2.4 cm inside

diameter) was driven into the river bed to a depth of ~60cm. N_2(l) was poured down the tube for ~15 minutes, until a sufficient quantity of material had frozen to the outside of the rod. The rod and attached material was removed from the river bed with a chain hoist suspended beneath a tripod. Profiles were placed over an aluminum foil lined cooler containing dry ice. Frozen material was removed by with a mallet. The material was then wrapped in the foil and transported on dry ice to storage at -80°C. In the lab, profiles were sectioned into 10cm depth intervals from 0-60 cm (n = 6 per profile, except for NV3 which was sectioned only from 30-60cm; total n = 33)

2.3. Physicochemistry

Details concerning physicochemical assays are provided in the Supporting Information. Briefly, we determined the particle distribution of sediments by separating size fractions via sieving; total nitrogen, sulfur, and carbon content were determined using an Elementar vario EL cube (Elementar Co.Germany); NH_4^+ was extracted with KCl and measured with Hach Kit 2604545 (Hach, Loveland, Co); iron content was measured with a ferrozine assay; and all other ion concentrations were measured by inductively coupled plasma mass spectrometry (ICP-MS) on HCl extractions. Aerobic metabolism was determined with a resazurin reduction assay, modified from *Haggerty et al.* [2009]

2.4. FT-ICR-MS solvent extraction and data acquisition

We leverage state of science chemical extraction protocols combined with Electrospray ionization (ESI) and Fourier transform ion cyclotron resonance (FT-ICR) mass spectrometry (MS) to infer differences in OC character among our samples. Previously, *Tfaily et al.* [2015;

2017] have demonstrated the optimization of OC characterization from soils and sediments by sequential extraction with polar and non-polar solvents tailored to the sample set of interest. Tfaily's extraction procedures have been coupled to ESI FT-ICR-MS to distinguish OC pools among ecosystems and soil types [*Malak M Tfaily et al.*, 2015; *M.M. Tfaily et al.*, 2017] as well as to provide information on the metabolism of distinct OC pools among samples within a single environment [*Bailey et al.*, 2017]. Other common OC characterization methods such as nuclear magnetic resonance spectroscopy (NMR), Fourier transform infrared spectroscopy (FT-IR), and gas chromatography MS only analyze a limited number of compound classes [*Kögel-Knabner*, 2002; *Kögel-Knabner*, 2000]. In contrast, ESI FT-ICR-MS introduces intact organic molecules into the MS without fragmentation and allows for the detection of a wide range of chemical compounds [*Malak M Tfaily et al.*, 2015; *M.M. Tfaily et al.*, 2017]. The use of 12 Tesla (T) FT-ICR-MS offers high mass resolving power (>1M) and mass measurement accuracy (<1 ppm), and while nascent in its application within complex environmental systems, it has emerged as a prevailing method for determining OC chemistry of natural organic matter [*Kim et al.*, 2003; *Koch et al.*, 2005; *Malak M Tfaily et al.*, 2011; *Tremblay et al.*, 2007]. Moreover, *Tfaily et al.* [2015; 2017] have demonstrated that sequential extraction with targeted solvents can preferentially select OC pools with differing chemical character (e.g., lipid-like vs. carbohydrate-like).

Here, we used three solvents with different polarities —water (H_2O), methanol (CH_3OH, hereafter "MeOH") and chloroform ($CHCl_3$)—to sequentially extract a large diversity of organic compounds from samples, according to *Tfaily et al.* [2015; 2017]. Water extractions were preformed first, followed by MeOH and then $CHCl_3$. Previous work has shown that each solvent is selective towards specific types of compounds [*Malak M Tfaily et al.*, 2015]. Water is a polar

159 solvent with a selection bias for carbohydrates with high O/C ratios, amino-sugars and other
160 labile polar compounds [*Malak M Tfaily et al.*, 2015]; and, as nearshore environments frequently
161 experience wetting, water extractions represent an estimation of readily accessible OC
162 compounds in these environments. Conversely, $CHCl_3$ is selective for non-polar lipids associated
163 with mineral interactions and cellular membranes (i.e., physically-bound OC) [*Malak M Tfaily et*
164 *al.*, 2015]. Because MeOH has a polarity in between that of water and $CHCl_3$, it extracts both
165 water-soluble and bound-OC pools (i.e., a mix of compounds that water and $CHCl_3$ extract), and
166 *Tfaily et al.* [2015] have demonstrated compositional overlap between water-soluble and MeOH
167 extracted OC pools. In this study, we are interested in the differences in OC composition
168 between pure water-soluble and bound-OC pools, and we will focus our discussion on H_2O- and
169 $CHCl_3$-extractions only. We use H_2O- and $CHCl_3$-extracted OC as proxies for readily
170 bioavailable (i.e., weakly bound) vs. less bioavailable (i.e., mineral- and microbial-bound) pools,
171 respectively.

172 Extracts were prepared by adding 1 ml of solvent to 100 mg bulk sediment and shaking in
173 2 mL capped glass vials for two hours on an Eppendorf Thermomixer. Samples were removed
174 from the shaker and left to stand before spinning down and pulling off the supernatant to stop the
175 extraction. The residual sediment was dried with nitrogen gas to remove any remaining solvent,
176 and then the next solvent was added. The $CHCl_3$ and H_2O extracts were diluted in MeOH to
177 improve ESI efficiency. *Tfaily et al.* [2015] estimated the OC extraction efficiency to be ~15%.
178 *Tfaily et al.* [2015] have previously demonstrated extraction efficiencies as low as 2% to be
179 representative of OC pool composition. We further note that numerous studies have established
180 FT-ICR-MS as a robust method for distinguishing compositional differences among OC pools

[*Herzsprung et al.*, 2017; *Kellerman et al.*, 2015; *Rossel et al.*, 2016; *Ward and Cory*, 2015; *Zhang et al.*, 2016].

Ultra-high resolution mass spectrometry of the three different extracts from each sample was carried out using a 12 Tesla Bruker SolariX FT-ICR-MS located at the Environmental Molecular Sciences Laboratory (EMSL) in Richland, WA, USA. As per *Tfaily at al.* [2017], we performed weekly calibration using a tuning solution containing C_2F_3O2, $C_6HF_9N_3O$, $C_{12}HF_{21}N_3O$, $C_{20}H_{18}F_{27}N_3O_8P_3$, and $C_{26}H_{18}F_{39}N_3O_8P_3$ with m/z ranging from 112 to 1333 (Agilent Technologies, Santa Clara, CA USA), and instrument settings were optimized using Suwannee River Fulvic Acid (IHSS). The instrument was flushed between samples using a mixture of water and methanol. Blanks were analyzed at the beginning and the end of the day to monitor for background contaminants.

The extracts were injected directly into the mass spectrometer and the ion accumulation time was optimized for all samples to account for differences in OC concentration. The ion accumulation time ranged between 0.5 and 1s. A standard Bruker electrospray ionization (ESI) source was used to generate negatively charged molecular ions. Samples were introduced to the ESI source equipped with a fused silica tube (30 μm i.d.) through an Agilent 1200 series pump (Agilent Technologies) at a flow rate of 3.0 μL min^{-1}. Experimental conditions were as follows: needle voltage, +4.4 kV; Q1 set to 50 *m*/*z*; and the heated resistively coated glass capillary operated at 180 °C.

2.5. FT-ICR-MS data processing

One hundred forty-four individual scans were averaged for each sample and internally calibrated using an organic matter homologous series separated by 14 Da ($–CH_2$ groups). The

mass measurement accuracy was less than 1 ppm for singly charged ions across a broad *m*/*z* range (100-1200 *m*/*z*). The mass resolution was ~ 350K at 339 m/z. Data Analysis software (BrukerDaltonik version 4.2) was used to convert raw spectra to a list of m/z values applying FTMS peak picker module with a signal-to-noise ratio (S/N) threshold set to 7 and absolute intensity threshold to the default value of 100.

Putative chemical formulae were then assigned using in-house built software following the Compound Identification Algorithm (CIA), proposed by *Kujawinski and Behn* [2006], modified by *Minor et al.* [2012], and previously described in *Tfaily et al.* [2017]. Chemical formulae were assigned based on the following criteria: S/N >7, and mass measurement error <1 ppm, taking into consideration the presence of C, H, O, N, S and P and excluding other elements. To ensure consistent formula assignment, we aligned all sample peak lists for the entire dataset to each other in order to facilitate consistent peak assignments and eliminate possible mass shifts that would impact formula assignment. We implemented the following rules to further ensure consistent formula assignment: (1) we consistently picked the formula with the lowest error and with the lowest number of heteroatoms and (2) the assignment of one phosphorus atom requires the presence of at least four oxygen atoms.

2.6. Identification of putative biochemical transformations using FT-ICR-MS

To identify potential biochemical transformation pathways, we followed the procedure detailed by *Breitling et al.* [2006] and employed by *Bailey et al.* [2017]. In essence, the mass difference between m/z peaks extracted from each spectrum with S/N>7 were compared to commonly observed mass differences associated with biochemical transformations. All possible pairwise mass differences were calculated within each extraction type, and differences (within

1ppm) were matched to a list of 92 common biochemical transformations (e.g., gain or loss of amino groups or sugars). For example, a mass difference of 99.07 corresponds to a gain or loss of the amino acid valine, while a difference of 179.06 corresponds to the transfer of a glucose molecule. Pairs of peaks with a mass difference within 1 ppm of our transformation list were considered to be related by the corresponding compound. This approach is feasible with FT-ICR-MS data because the set of peaks in each sample are related by measureable and clearly defined mass differences corresponding to gains and losses of compounds. It has been previously used by *Bailey et al.* [2017] to demonstrate differences in biochemical transformations among soils incubated with different microbial inoculate and among pore size classes in complex soil matrices.

2.7. Identification of putative microbial metabolic pathways using FT-IR-MS

Additionally, a set of putative microbial metabolic pathways in each sample can be identified by locating chemical formulae assigned to m/z's within metabolic pathways defined in the Kyoto Encyclopedia of Genes and Genomes (KEGG, Release, 80.0, http://www.kegg.jp) [*Kanehisa and Goto*, 2000]. For example, a peak with a mass of 400.3356 was assigned formula $C_{20}H_{16}O_9$ and mapped to KEGG pathway 'map00254' (Aflatoxin biosynthesis). While only a subset of compounds detected by FT-ICR-MS are defined within the KEGG database (i.e., peaks must be assigned a chemical formula and that chemical formula must be present in a KEGG pathway), we found 415 unique peaks that were assigned putative molecular formulae *and* that corresponded to compounds present in KEGG pathways. Additionally, we defined assignments at the pathway level (i.e., by "map" number) instead of using enzyme level classification (i.e.,

EC number) in order to aggregate compounds found within the same pathways. This was done to facilitate functional interpretation.

Although we acknowledge our results do not represent a comprehensive analysis of all microbial metabolic pathways present in a sample, we assume that KEGG pathways containing more peaks detected by FT-ICR-MS within a sample are more likely to be active than those with fewer mapped peaks. We further reduced possible random matches by assessing correlations with aerobic metabolisms as described in the 'Statistical Methods' section below, and we compare results across samples to yield insight into microbial pathways in each sample beyond that which can be garnered from biochemical transformations. The results are, however, conceptually congruent with those derived from the biochemical transformation analyses described in the preceding sub-section. The KEGG pathway and transformation analyses are independent of each other, yet provided consistent insights and thus together they provide greater confidence in our interpretations.

2.8. Statistical Methods

All statistical analyses were conducted using R software (https://www.r-project.org/). FT-ICR m/z intensities were converted into presence/absence data prior to analysis because differences in m/z intensity are influenced by ionization efficiency as well as relative abundance [*Kujawinski and Behn*, 2006; *Minor et al.*, 2012; *Malak M Tfaily et al.*, 2015; *M.M. Tfaily et al.*, 2017].

To examine differences in OC composition between transects, we used the 'vegan' package to construct a Sorenson dissimilarity matrix for all m/z's identified (i.e., we included peaks with or without assigned formula) within each OC pool (water-soluble or physically-

bound). Differences between vegetation states (i.e., V vs. NV) were tested with PERMANOVA (999 permutations, 'vegan') and visualized using Non-metric Multidimensional Scaling (NMDS, 'vegan'). One sample (NV, profile 1, depth 30-40cm) was removed due to peak interference during FT-ICR-MS, and three samples (NV, profile 2, depths 00-10cm, 10-20cm, 20-30cm) were excluded because were unable to collect sufficient sample mass for all analyses.

To reveal transformations associated with aerobic metabolism and to study differences in those transformations across vegetation states, we determined the number of times a given transformation occurred within each OC pool in each sample. Specifically, for each of the 92 compounds in our set of biochemical transformations, we counted the number of times in each sample that transformation was observed to yield an estimate of the prevalence or 'abundance' of each transformation in each sample. We correlated these abundance estimates to rates of metabolism using Pearson's product-moment correlation coefficient. Positive relationships were inferred as biochemical transformations possibly associated with biotic OC oxidation. To determine variation in biochemical transformations across vegetation states, we calculated Bray-Curtis dissimilarity from the abundance of biochemical transformations that positively correlated with aerobic metabolism at either vegetation state, visualized them with non-metric Multidimensional Scaling visualization (NMDS, 'vegan'), and statistically evaluated them with PERMANOVA (999 permutations, 'vegan'). We refer to H_2O- and $CHCl_3$-soluble OC pools at V and NV, respectively, as V-W ('vegetated water'), V-B ('vegetated bound'), NV-W ('not vegetated water'), and NV-B ('not vegetated bound') for the remainder of the manuscript.

Similar to our analyses of biochemical transformations, we found the number of m/z's that mapped to a given KEGG pathway. We make the assumption that pathways with more m/z's mapped to them have a higher probability of actively contributing to biogeochemical function.

To identify which pathways were most likely to contribute to aerobic metabolism, we correlated the number of m/z's mapped to a given KEGG pathway within each sample to aerobic metabolism. Those pathways with positive correlations were interpreted as contributing to OC oxidation, and the following analysis was conducted only with positively correlated KEGG pathways. The number peaks mapping to each KEGG pathway in a sample was normalized by the total number of peaks mapping to any positively correlated KEGG pathway in the sample to yield data as a relative abundance. Pathways were clustered based on their relative abundance in each vegetation state and pool type. Clusters were determined using the 'hclust' algorithm in R with the 'complete linkage' clustering method and visualized using the 'pheatmap' package.

Finally, we examined associations between aerobic metabolism and OC thermodynamics by calculating the Gibbs Free Energy of OC oxidation under standard conditions (ΔG^{o}_{Cox}) from the Nominal Oxidation State of Carbon (NOSC) as per *La Rowe and Van Cappellen* [2011]. NOSC was calculated from the number of electrons transferred in OC oxidation half reactions and is defined by the equation:

$$(1)\quad NOSC = -((-Z + 4a + b - 3c - 2d + 5e - 2f)/a) + 4$$

, where a, b, c, d, e, and f are, respectively, the numbers of C, H, N, O, P, S atoms in a given organic molecule and Z is net charge of the organic molecule (assumed to be 1). In turn, ΔG^{o}_{Cox} was estimated from NOSC following *La Rowe and Van Cappellen* [2011]:

$$(2)\quad \Delta G^{o}_{Cox} = 60.3 - 28.5(NOSC)$$

Values of ΔG^{o}_{Cox} are generally positive, indicating that OC oxidation must be coupled to the reduction of a terminal electron acceptor. While ΔG^{o}_{Cox} varies according to the availability of terminal electron acceptors, our system is primarily oxic, allowing us to infer oxygen as the primary electron acceptor in most reactions and make direct comparisons across samples.

318 Additionally, though the exact calculation of ΔG^{o}_{Cox} necessitates an accurate quantification of all
319 species involved in every chemical reaction in a sample, the use of NOSC as a practical basis for
320 determining ΔG^{o}_{Cox} has been validated [*Arndt et al.*, 2013; *LaRowe and Van Cappellen*, 2011].
321 Here, we assessed relationships between aerobic metabolism and ΔG^{o}_{Cox} of OC
322 compounds identified in each OC pool (determined by FT-ICR-MS analysis) using linear
323 regressions in each vegetation state, in which aerobic metabolism (determined by resazurin
324 assay) was the independent variable and average ΔG^{o}_{Cox} of all m/z's with assigned formula was
325 the dependent variable.
326

327 **3. Results and Discussion**

328 *3.1. Shifts in physicochemical, metabolic, and OC character between vegetation states*

329 Differences in vegetation states corresponded to differences in physicochemistry, aerobic
330 metabolism, and OC pool composition. V was characterized by mature trees near the water line
331 and was nutrient-rich relative to NV (Figure S1-3). V displayed comparatively high
332 concentrations of total C and rates of aerobic metabolism (Figure S1-3). In contrast, NV
333 consisted of vegetation-free, cobble-ridden shoreline with sandier soils, low total C, and low
334 aerobic metabolism (Figure S1-3).
335 Compositional difference in OC pools indicated a possibility for distinct OC oxidation
336 processes between the vegetation states (Figure 1), as preferential oxidation of certain OC
337 compounds in each state would be expected to generate an observable difference in OC pool
338 composition. Further, total organic OC content explained only 38% of aerobic metabolic rates
339 ($R^2 = 0.38$, $P < 0.0001$, Figure S4), leaving open the possibility that OC compositional

differences may be related to differences in aerobic metabolism at each vegetation state. The following sections explore this possibility.

3.2. Associations between C transformations and aerobic metabolism

Given compositional differences in OC between vegetation states and known impacts of C chemistry on metabolic functioning in other systems [*Castle et al.*, 2016; *Graham et al.*, 2016b], we hypothesized that biochemical transformations related to rates of aerobic metabolism would be unique to each vegetation state.

Consistent with this hypothesis, transformation analysis indicated that the biochemical processes associated with OC oxidation were significantly different between the vegetation states. Specifically, OC transformations that increased in abundance with increases in aerobic metabolism were significantly different at each vegetation state (PERMANOVA, H_2O $P = 0.022$ and $CHCl_3$ $P = 0.002$, Figure 3 a-b, Table 2). In comparing differences in transformations occurring within the water-soluble OC pool, we observed higher abundances of amino- and sugar-associated transformations for V-W relative to NV-W. Twenty-six of these transformations were identified as contributing to aerobic metabolism in V-W, while none were identified in NV-W. These V-W transformations were primarily associated with simple C molecules (e.g., glucose, alanine, and lysine, Table 2). Conversely, within the bound-OC pool, 38 transformations were identified as contributing to aerobic metabolism in NV-B, compared to only 11 in V-B. In both cases, these transformations consisted of a greater proportion of complex C molecules (e.g., pyridoxal phosphate, palmitic acid, and glyoxylate, Table 2) than in water-soluble pools.

362 The larger number of transformations associated with aerobic metabolism in V-W vs. V-
363 B, and the larger number in NV-B vs. NV-W, suggests that aerobic metabolism in vegetated and
364 unvegetated areas depend on water-soluble and bound-OC pools, respectively. We note some
365 oxidation of the bound-OC pool under vegetated conditions, but only 11 correlations were
366 observed between V-B transformations and aerobic metabolism suggesting a relatively minor
367 role, especially considering that there were 38 significant correlations for NV-B. These
368 differences suggests that an increased supply of bioavailable compounds in vegetated areas leads
369 to bound-OC being less involved in aerobic metabolism, relative to unvegetated areas where
370 bound-OC appears to be heavily involved in aerobic metabolism. The concept of priming
371 [*Kuzyakov*, 2010] would predict the opposite pattern—a greater supply of bioavailable OC
372 should increase the contributions of less bioavailable OC (here, bound-OC) to aerobic
373 metabolism. Our results run counter to a priming mechanism and indicate that the supply of
374 bioavailable compounds—associated with riparian vegetation—diminishes the contribution of
375 bound-OC to aerobic metabolism and, in turn, protects bound-OC pools. Mineral-stabilized OC
376 therefore has greater potential to remain sequestered along river corridors with spatially and
377 temporally consistent inputs of bioavailable OC, potentially derived from riparian vegetation.
378 The fate of OC that moves across the terrestrial-aquatic continuum may therefore be impacted by
379 land use change [*Foley et al.*, 2005] in ways not currently represented in ESMs.
380
381 *3.3. Associations between microbial metabolic pathways and aerobic metabolism*
382 Because we observed stark differences in the identity of OC transformations that
383 correlated with aerobic metabolism across vegetation states, we hypothesized that the microbial
384 metabolic pathways associated with OC transformations were also dependent on vegetation state.

Indeed, pathways associated with OC oxidation were distinct at V vs. NV, supporting our hypothesis that there were differences in the metabolic processing of OC in the presence or absence of riparian vegetation. Specifically, while the metabolism of plant-derived compounds appeared to be a major driver of aerobic respiration at both vegetation states, metabolism at V mostly involved readily bioavailable plant derivatives in the water-soluble OC pool, and metabolism at NV was associated with plant derivatives in the bound-OC pool (Figure 4).

In V-W, two primary pathways were involved in metabolism of plant compounds, each contained within its own hierarchical cluster (map01110: Biosynthesis of secondary metabolites; map00941: Flavonoid biosynthesis). A concomitant cluster of plant-associated metabolisms with lower abundance in V-W (Cluster 4) was also positively correlated to aerobic metabolism (Figure 4). Secondary metabolites (map01110) are largely comprised of plant-derived compounds such as flavonoids [*Agati et al.*, 2012], terpenoids [*Tholl*, 2015], and nitrogen-containing alkaloids [*Willaman and Schubert*, 1961], while flavonoids [*Agati et al.*, 2012] are one of those most abundant plant-derived compounds. Associations with aflatoxin [*Trail et al.*, 1995], flavone/flavonol [*Agati et al.*, 2012], and phenylpropanoids [*Hahlbrock and Scheel*, 1989] (Cluster 4) bolster this association between plant-associated metabolic pathways and aerobic metabolism in V-W.

Although correlations between plant-associated KEGG pathways and aerobic metabolism could indicate the persistence of plant secondary metabolites rather than microbial metabolism, our results indicate a central role for vegetation in water-soluble OC oxidation in either case. For example, if KEGG associations were attributable to plant metabolism instead of microbial metabolism, correlations between plant-associated pathways and aerobic metabolism in V-W would indicate an indirect relationship between plant growth and microbial oxidation of OC,

whereby plant byproducts support microbial communities in oxidizing other portions of the OC pool.

In contrast to V-W, NV-W did not display associations between plant-associated metabolic pathways and OC oxidation. All correlations indicated broad metabolic processes including membrane transport and carbohydrate metabolism that may indicate utilization of other resources (Cluster 3, Figure 4).

Instead, we observed relationships between plant-associated metabolisms and OC oxidation within NV-B. For example, correlations were strongest in Cluster 1, which contained pathways of cutin, suberine, and wax biosynthesis [*King et al.*, 2007; *Raffaele et al.*, 2009; *Shepherd and Wynne Griffiths*, 2006], alpha-linolenic acid metabolism [*Crawford et al.*, 2000; *Creelman and Mulpuri*, 2002], and biosynthesis of secondary metabolites [*Agati et al.*, 2012; *Tholl*, 2015; *Willaman and Schubert*, 1961] (Figure 4). Each of these pathways denotes the synthesis or metabolism of a plant-associated lipid compound. Because no specific metabolisms were correlated to OC oxidation in the water-soluble pool, we hypothesize that these lipid-based metabolisms comprise the primary KEGG-identifiable pathways associated with OC oxidation in areas without riparian vegetation. We also observed one cluster of pathways that correlated with metabolism at V-B (Cluster 7) and contained plant-associated metabolic pathways such as linoleic acid metabolism [*Crawford et al.*, 2000; *Creelman and Mulpuri*, 2002] and brassinosteroid biosynthesis [*Bishop*, 2007], indicating some oxidation of lipid plant material in the bound-OC pool under vegetated conditions. We therefore propose that plant-derived lipid compounds serve as a secondary substrate for OC oxidation in shorelines with riparian vegetation, given that most correlations at V were detected in the water-soluble pool.

3.4. Thermodynamics of carbon oxidation

Finally, we hypothesized that microbes would preferentially oxidize more thermodynamically favorable compounds at both sites, consistent with common thermodynamic constraints on biogeochemical cycles [*Burgin et al.*, 2011; *Hedin et al.*, 1998; *Helton et al.*, 2015]. Because we observed evidence for preferential OC oxidation of the water-soluble OC pool at V and of the bound-OC pool at NV, we further hypothesized that thermodynamic-based preference of OC oxidation would be observable only in the preferred substrate pool within each vegetation state. Consistent with this hypothesis, aerobic metabolism was positively correlated to average ΔG^{o}_{Cox} in V-W ($R^2 = 0.22$, $P = 0.03$, Fig 5a) and NV-B ($R^2 = 0.54$, $P = 0.001$ Fig 5b), but these variables were not correlated in V-B or NV-W. In both cases, aerobic metabolism corresponded to a depletion of more thermodynamically favorable OC (i.e., OC became less favorable as aerobic metabolism increased), resulting in progressively less favorable thermodynamic conditions.

The priming conceptual framework would predict that terrestrial inputs associated with riparian vegetation should condition microbial communities to oxidize less thermodynamically favorable C, such as that found in the bound-OC pool. In such a scenario, inputs of thermodynamically favorable carbon should—by minimizing community-level energy constraints—allow for the rise of microbial physiologies that can oxidize less favorable C [*Kuzyakov*, 2010]. In this case, a significant relationship between thermodynamic favorability and aerobic metabolism in the V-W pool should lead to a similar relationship within the V-B pool. Our results reveal a strong relationship within the V-W pool, but not in the V-B pool, thereby rejecting an influence of priming. Instead, our results suggest that bound-OC pools are protected by thermodynamically favorable compounds that serve as preferred substrate.

In contrast to our expectation that water-soluble OC associated with riparian vegetation would increase oxidation of bound-OC pools, we observed evidence consistent with inhibition of bound-OC oxidation by thermodynamically favorable water-soluble compounds. Priming has been actively debated in aquatic research [*Bengtsson et al.*, 2014; *Bianchi*, 2011; *Guenet et al.*, 2010], and a number of other studies have been unable to detect a priming effect in sediment and aqueous habitats [*Bengtsson et al.*, 2014; *Catalán et al.*, 2015].

The mechanisms resulting in priming are not well understood, but the phenomenon has been associated with nutrient and energy limitations in soil environments [*Kuzyakov*, 2010]. For instance, under nutrient limitation microorganisms may oxidize chemically-complex OC to garner resources (e.g., nitrogen mining), while shared resources that facilitate OC oxidation (e.g., extracellular enzymes) are more likely to facilitate ecological cheating under energy limiting conditions [*Blagodatskaya and Kuzyakov*, 2008; *Catalán et al.*, 2015; *Guenet et al.*, 2010; *Kuzyakov*, 2010]. Our system is oligotrophic, containing a fraction of the total C content observed in other systems (Figure S1) such that C limitation rather than nutrient limitation might drive OC oxidation dynamics. In such a case, readily bioavailable C inputs would be rapidly oxidized but microbial communities may be well-adapted to rely on alternative energy sources (e.g., NH_4^+, Fe) that may be more available than bound-OC pools.

3.5. Conceptual model for OC oxidation at terrestrial-aquatic interfaces

Based on our work, we propose a conceptual model of OC oxidation along terrestrial-aquatic interfaces in which the oxidation of bound-OC is limited by terrestrial inputs from riparian vegetation (Fig 6. a-b). Riparian vegetation sustains inputs of water-soluble compounds to nearshore OC pools, resulting in a larger thermodynamically favorable, water-soluble OC pool

(Figure 6b). This leads to higher overall C content in nearshore sediments and elevated rates of aerobic respiration relative to areas with less riparian vegetation. However, our data suggest that in the presence of riparian vegetation microbial carbon oxidation primarily uses the water-soluble OC pool with minimal oxidation of bound-OC due to physical and/or thermodynamic protection of this pool. For instance, ΔG^{o}_{Cox} was lower in water-soluble OC pools than in bound-OC, and a large presence of this thermodynamically favorable pool may provide adequate substrate to sustain metabolic functioning, limiting the need to metabolize less thermodynamically favorable OC. Additionally, organomineral interactions can protect bound-OC from extracellular enzyme acitivity [*Hunter et al.*, 2016], inhibiting the bioavailability of OC by sequestering it within larger aggregates.

In contrast, non-vegetated riparian zones provide little input into water-soluble OC pools (Fig 6a), and rates of metabolism and C pool sizes are lower in these environments. Carbon oxidation in these non-vegetated zones occurs primarily within the bound-OC pool, albeit more slowly and as product of different biochemical and metabolic pathways than in vegetated environments (e.g., complex C transformations and lipid-based metabolism of plant derivatives). We posit that water-soluble pools in non-vegetated sediments are sufficiently small that investing in enzymes needed to metabolize this OC pool results in a net energy loss. Instead, microbes in unvegetated areas must investment in cellular machinery to access bound-OC, and our results imply that the cellular machinery needed to access bound-OC is distinct from the machinery needed to access water-soluble OC.

Interestingly, aerobic metabolism within both types of sediments is related to a depletion of thermodynamically favorable compounds; however, this dynamic is associated with water-soluble OC pools in vegetated zones vs. bound-OC pools in non-vegetated zones. That is,

microorganisms in both environments are constrained to the metabolism of their primary substrate pool but preferentially oxidize more thermodynamically favorable compounds within that pool. This dynamic suggests that microorganisms are conditioned to metabolize a subset of compounds within sediment OC, possibly defined by thermodynamic or physical protection mechanisms, but operate under common thermodynamic constraints once adapted to oxidize a certain OC pool.

3.6. Broader Implications

Our results indicate that terrestrial C inputs associated with riparian vegetation protect bound-OC from oxidation, possibly aiding long-term storage of mineral-bound pools along river corridors, and our work is particularly relevant to global patterns of CO_2 emissions in light of changes in land cover and increases in C fluxes across the terrestrial-aquatic interface. The magnitude, distribution, and chemical quality of terrestrial C fluxes into aquatic environments are perturbed by shifts in land cover (e.g., due to agriculture, urbanization, and climate-driven vegetation change) [*Fang et al.*, 2005; *Knapp et al.*, 2008]. These fluxes have been examined primarily for their own propensity to be oxidized along land-to-sea continuums [*Battin et al.*, 2008; *Battin et al.*, 2009; *Regnier et al.*, 2013], but we also suggest a role for these fluxes in stabilizing mineral-bound carbon within nearshore environments. For example, vegetation removal, impervious surfaces, and drainage systems coincident with urbanization alter terrestrial C runoff patterns, both changing their magnitude and creating preferential deposition flowpaths [*Fraley et al.*, 2009; *Imberger et al.*, 2011; *Smith and Kaushal*, 2015]. Agricultural drainage systems also lead to preferential flowpaths as well as spatiotemporal variation in the quantity and quality of terrestrial-aquatic fluxes [*Graeber et al.*, 2012; *Larson et al.*, 2014], an effect that

strongly influences C cycling given that 40% of the earth's land is cultivated [*Foley et al.*, 2005; *Graeber et al.*, 2012]. We propose that changes in the distribution of these fluxes through space and time may impact OC oxidation both in the C transported along these flow paths and within sediments that are differentially exposed to terrestrial OC.

Furthermore, vegetation distributions in natural ecosystems are predicted to shift in response to altered precipitation regimes. Associated changes in plant phenology, morphology, and establishment will impact the quantity, quality, and distribution of terrestrial material entering aquatic systems [*Knapp et al.*, 2008], and we currently have an incomplete understanding of how these patterns will vary across ecosystems and precipitation patterns [*Fang et al.*, 2005; *Knapp et al.*, 2008]. A mechanistic framework for C oxidation that captures impacts of heterogeneity in vegetation in river corridors will therefore aid in predicting how terrestrial-aquatic interfaces respond to ongoing perturbations. Here, we demonstrate a potential for increases in the intensity of terrestrial C fluxes to lead to larger mineral-bound C pools by physically and thermodynamically protecting these pools; and conversely, a potential for oxidation of mineral-bound C pools in areas with diminished terrestrial C inputs.

Earth System Models depend on mathematical representations of C cycling, and the continued development of these models is tightly coupled to conceptual advances drawn from field-based observations [*Burd et al.*, 2016; *Six et al.*, 2002]. Despite recent progress, these models are still missing key regulatory processes [*Todd-Brown et al.*, 2013; *Wieder et al.*, 2013; *Wieder et al.*, 2015]. To address this knowledge gap, we propose a new conceptual framework of OC dynamics based on analysis of *in situ* observational data that explicitly considers a central challenge in model improvement—biochemical, metabolic, and thermodynamic mechanisms governing OC oxidation along terrestrial-aquatic interfaces. Our results directly contrast those

546 expected within a 'priming' framework, and we advance that water-soluble thermodynamically
547 favorable OC associated with riparian vegetation protects thermodynamically less favorable
548 bound-OC from oxidation. We also demonstrate differences in biochemical and metabolic
549 pathways associated with metabolism of water-soluble and bound-OC pools in the presence or
550 absence of riparian vegetation, furthering a processed-based understanding of terrestrial-aquatic
551 interfaces.

552 Our conceptualization of OC oxidation may also be applicable beyond terrestrial-aquatic
553 interfaces, as many ecosystems experience spatiotemporal variability in the quantity of
554 thermodynamically favorable water-soluble OC. For instance, vegetation senescence generates
555 pulses of bioavailable C into most temperate and tropical ecosystems. Our research provides an
556 opportunity to enhance the mechanistic underpinning of OC oxidation process representations
557 within ESMs—an imperative under heterogeneous landscapes and unknown future land cover
558 distributions—and proposes interactions between OC thermodynamics and mineral-inhibition of
559 OC oxidation as a key future research need.

560

561 **Author Contributions.**

562 EBG was responsible for conceptual development and data analysis and was the primary writer
563 with guidance from JCS and MT. ARC, AEG, CTR, ECR, DWK, and JCS were responsible for
564 experimental design and data collection. MT was responsible for all FT-ICR processing. All
565 authors contributed to manuscript revisions.

566

567 **Acknowledgements.**

568 This research was supported by the US Department of Energy (DOE), Office of

569 Biological and Environmental Research (BER), as part of Subsurface Biogeochemical
570 Research Program's Scientific Focus Area (SFA) at the Pacific Northwest National
571 Laboratory (PNNL). PNNL is operated for DOE by Battelle under contract
572 DE-AC06-76RLO 1830. A portion of the research was performed at Environmental Molecular
573 Science Laboratory User Facility. We thank Nancy Hess for helpful feedback in manuscript
574 revision.

575

576 **References.**
577
578 Aalto, R., L. Maurice-Bourgoin, T. Dunne, D. R. Montgomery, C. A. Nittrouer, and J.-L. Guyot
579 (2003), Episodic sediment accumulation on Amazonian flood plains influenced by El
580 Nino/Southern Oscillation, *Nature*, *425*(6957), 493-497.
581 Agati, G., E. Azzarello, S. Pollastri, and M. Tattini (2012), Flavonoids as antioxidants in plants:
582 location and functional significance, *Plant Science*, *196*, 67-76.
583 Arndt, S., B. B. Jørgensen, D. E. LaRowe, J. Middelburg, R. Pancost, and P. Regnier (2013),
584 Quantifying the degradation of organic matter in marine sediments: a review and synthesis,
585 *Earth-science reviews*, *123*, 53-86.
586 Arntzen, E. V., D. R. Geist, and P. E. Dresel (2006), Effects of fluctuating river flow on
587 groundwater/surface water mixing in the hyporheic zone of a regulated, large cobble bed river,
588 *River Research and Applications*, *22*(8), 937-946.
589 Bailey, V. L., A. Smith, M. Tfaily, S. J. Fansler, and B. Bond-Lamberty (2017), Differences in
590 soluble organic carbon chemistry in pore waters sampled from different pore size domains, *Soil*
591 *Biology and Biochemistry*, *107*, 133-143.
592 Battin, T. J., L. A. Kaplan, S. Findlay, C. S. Hopkinson, E. Marti, A. I. Packman, J. D. Newbold,
593 and F. Sabater (2008), Biophysical controls on organic carbon fluxes in fluvial networks, *Nature*
594 *Geoscience*, *1*(2), 95-100.
595 Battin, T. J., S. Luyssaert, L. A. Kaplan, A. K. Aufdenkampe, A. Richter, and L. J. Tranvik
596 (2009), The boundless carbon cycle, *Nature Geoscience*, *2*(9), 598-600.
597 Bengtsson, M. M., K. Wagner, N. R. Burns, E. R. Herberg, W. Wanek, L. A. Kaplan, and T. J.
598 Battin (2014), No evidence of aquatic priming effects in hyporheic zone microcosms, *Scientific*
599 *reports*, *4*, 5187.
600 Bianchi, T. S. (2011), The role of terrestrially derived organic carbon in the coastal ocean: A
601 changing paradigm and the priming effect, *Proceedings of the National Academy of Sciences*,
602 *108*(49), 19473-19481.
603 Bishop, G. J. (2007), Refining the plant steroid hormone biosynthesis pathway, *Trends in plant*
604 *science*, *12*(9), 377-380.
605 Blagodatskaya, E., and Y. Kuzyakov (2008), Mechanisms of real and apparent priming effects
606 and their dependence on soil microbial biomass and community structure: critical review,
607 *Biology and Fertility of Soils*, *45*(2), 115-131.
608 Breitling, R., S. Ritchie, D. Goodenowe, M. L. Stewart, and M. P. Barrett (2006), Ab initio
609 prediction of metabolic networks using Fourier transform mass spectrometry data,
610 *Metabolomics*, *2*(3), 155-164.
611 Burd, A. B., S. Frey, A. Cabre, T. Ito, N. M. Levine, C. Lønborg, M. Long, M. Mauritz, R. Q.
612 Thomas, and B. M. Stephens (2016), Terrestrial and marine perspectives on modeling organic
613 matter degradation pathways, *Global change biology*, *22*(1), 121-136.
614 Burgin, A. J., W. H. Yang, S. K. Hamilton, and W. L. Silver (2011), Beyond carbon and
615 nitrogen: how the microbial energy economy couples elemental cycles in diverse ecosystems,
616 *Frontiers in Ecology and the Environment*, *9*(1), 44-52.
617 Castle, S. C., D. R. Nemergut, A. S. Grandy, J. W. Leff, E. B. Graham, E. Hood, S. K. Schmidt,
618 K. Wickings, and C. C. Cleveland (2016), Biogeochemical drivers of microbial community
619 convergence across actively retreating glaciers, *Soil Biology and Biochemistry*, *101*, 74-84.

620 Catalán, N., A. M. Kellerman, H. Peter, F. Carmona, and L. J. Tranvik (2015), Absence of a
621 priming effect on dissolved organic carbon degradation in lake water, *Limnology and*
622 *Oceanography*, *60*(1), 159-168.
623 Cotrufo, M. F., M. D. Wallenstein, C. M. Boot, K. Denef, and E. Paul (2013), The Microbial
624 Efficiency‐Matrix Stabilization (MEMS) framework integrates plant litter decomposition with
625 soil organic matter stabilization: do labile plant inputs form stable soil organic matter?, *Global*
626 *Change Biology*, *19*(4), 988-995.
627 Crawford, M., C. Galli, F. Visioli, S. Renaud, A. P. Simopoulos, and A. A. Spector (2000), Role
628 of plant-derived omega–3 fatty acids in human nutrition, *Annals of Nutrition and Metabolism*,
629 *44*(5-6), 263-265.
630 Creelman, R. A., and R. Mulpuri (2002), The oxylipin pathway in Arabidopsis, *The Arabidopsis*
631 *Book*, e0012.
632 Dorado-García, I., J. Syväranta, S. P. Devlin, J. M. Medina-Sánchez, and R. I. Jones (2016),
633 Experimental assessment of a possible microbial priming effect in a humic boreal lake, *Aquatic*
634 *Sciences*, *78*(1), 191-202.
635 Ebel, W. J., C. D. Becker, J. W. Mullan, and H. L. Raymond (1989), The Columbia River--
636 toward a holistic understanding, *Canadian special publication of fisheries and aquatic*
637 *sciences/Publication speciale canadienne des sciences halieutiques et aquatiques. 1989*.
638 Fang, J., S. Piao, L. Zhou, J. He, F. Wei, R. B. Myneni, C. J. Tucker, and K. Tan (2005),
639 Precipitation patterns alter growth of temperate vegetation, *Geophysical research letters*, *32*(21).
640 Foley, J. A., R. DeFries, G. P. Asner, C. Barford, G. Bonan, S. R. Carpenter, F. S. Chapin, M. T.
641 Coe, G. C. Daily, and H. K. Gibbs (2005), Global consequences of land use, *science*, *309*(5734),
642 570-574.
643 Fraley, L. M., A. J. Miller, and C. Welty (2009), Contribution of In‐Channel Processes to
644 Sediment Yield of an Urbanizing Watershed1, *JAWRA Journal of the American Water Resources*
645 *Association*, *45*(3), 748-766.
646 Graeber, D., J. Gelbrecht, M. T. Pusch, C. Anlanger, and D. von Schiller (2012), Agriculture has
647 changed the amount and composition of dissolved organic matter in Central European headwater
648 streams, *Science of the Total Environment*, *438*, 435-446.
649 Graham, E. B., A. R. Crump, C. T. Resch, S. Fansler, E. Arntzen, D. W. Kennedy, J. K.
650 Fredrickson, and J. C. Stegen (2016a), Coupling spatiotemporal community assembly processes
651 to changes in microbial metabolism, *Frontiers in Microbiology*, *7*, 1949.
652 Graham, E. B., A. R. Crump, C. T. Resch, S. Fansler, E. Arntzen, D. W. Kennedy, J. K.
653 Fredrickson, and J. C. Stegen (2017), Deterministic influences exceed dispersal effects on
654 hydrologically‐connected microbiomes, *Environmental Microbiology*, *19*(4), 1552-1567.
655 Graham, E. B., J. E. Knelman, R. S. Gabor, S. Schooler, D. M. McKnight, and D. Nemergut
656 (2016b), Dissolved organic matter and inorganic mercury loadings favor novel methylators and
657 fermentation metabolisms in oligotrophic sediments, *bioRxiv*, 072017.
658 Guenet, B., M. Danger, L. Abbadie, and G. Lacroix (2010), Priming effect: bridging the gap
659 between terrestrial and aquatic ecology, *Ecology*, *91*(10), 2850-2861.
660 Haggerty, R., E. Martí, A. Argerich, D. Von Schiller, and N. B. Grimm (2009), Resazurin as a
661 “smart” tracer for quantifying metabolically active transient storage in stream ecosystems,
662 *Journal of Geophysical Research: Biogeosciences*, *114*(G3).
663 Hahlbrock, K., and D. Scheel (1989), Physiology and molecular biology of phenylpropanoid
664 metabolism, *Annual review of plant biology*, *40*(1), 347-369.

Hedges, J., and J. Oades (1997), Comparative organic geochemistries of soils and marine sediments, *Organic geochemistry*, *27*(7), 319-361.

Hedges, J. I., G. Eglinton, P. G. Hatcher, D. L. Kirchman, C. Arnosti, S. Derenne, R. P. Evershed, I. Kögel-Knabner, J. De Leeuw, and R. Littke (2000), The molecularly-uncharacterized component of nonliving organic matter in natural environments, *Organic Geochemistry*, *31*(10), 945-958.

Hedges, J. I., and R. G. Keil (1995), Sedimentary organic matter preservation: an assessment and speculative synthesis, *Marine chemistry*, *49*(2-3), 81-115.

Hedin, L. O., J. C. von Fischer, N. E. Ostrom, B. P. Kennedy, M. G. Brown, and G. P. Robertson (1998), Thermodynamic constraints on nitrogentransformations and other biogeochemicalprocesses at soil–stream interfaces, *Ecology*, *79*(2), 684-703.

Helton, A. M., M. Ardón, and E. S. Bernhardt (2015), Thermodynamic constraints on the utility of ecological stoichiometry for explaining global biogeochemical patterns, *Ecology letters*, *18*(10), 1049-1056.

Herzsprung, P., K. Osterloh, W. von Tümpling, M. Harir, N. Hertkorn, P. Schmitt-Kopplin, R. Meissner, S. Bernsdorf, and K. Friese (2017), Differences in DOM of rewetted and natural peatlands–Results from high-field FT-ICR-MS and bulk optical parameters, *Science of The Total Environment*, *586*, 770-781.

Hunter, W. R., R. Niederdorfer, A. Gernand, B. Veuger, J. Prommer, M. Mooshammer, W. Wanek, and T. J. Battin (2016), Metabolism of mineral‐sorbed organic matter and microbial lifestyles in fluvial ecosystems, *Geophysical Research Letters*.

Imberger, S. J., R. M. Thompson, and M. R. Grace (2011), Urban catchment hydrology overwhelms reach scale effects of riparian vegetation on organic matter dynamics, *Freshwater Biology*, *56*(7), 1370-1389.

Kanehisa, M., and S. Goto (2000), KEGG: kyoto encyclopedia of genes and genomes, *Nucleic acids research*, *28*(1), 27-30.

Kellerman, A. M., D. N. Kothawala, T. Dittmar, and L. J. Tranvik (2015), Persistence of dissolved organic matter in lakes related to its molecular characteristics, *Nature Geoscience*, *8*(6), 454-457.

Kim, S., R. W. Kramer, and P. G. Hatcher (2003), Graphical method for analysis of ultrahigh-resolution broadband mass spectra of natural organic matter, the van Krevelen diagram, *Analytical Chemistry*, *75*(20), 5336-5344.

King, A., J.-W. Nam, J. Han, J. Hilliard, and J. G. Jaworski (2007), Cuticular wax biosynthesis in petunia petals: cloning and characterization of an alcohol-acyltransferase that synthesizes wax-esters, *Planta*, *226*(2), 381-394.

Knapp, A. K., C. Beier, D. D. Briske, A. T. Classen, Y. Luo, M. Reichstein, M. D. Smith, S. D. Smith, J. E. Bell, and P. A. Fay (2008), Consequences of more extreme precipitation regimes for terrestrial ecosystems, *Bioscience*, *58*(9), 811-821.

Koch, B. P., M. Witt, R. Engbrodt, T. Dittmar, and G. Kattner (2005), Molecular formulae of marine and terrigenous dissolved organic matter detected by electrospray ionization Fourier transform ion cyclotron resonance mass spectrometry, *Geochimica et Cosmochimica Acta*, *69*(13), 3299-3308.

KoÈgel-Knabner, I. (2002), The macromolecular organic composition of plant and microbial residues as inputs to soil organic matter, *Soil Biology and Biochemistry*, *34*(2), 139-162.

Kögel-Knabner, I. (2000), Analytical approaches for characterizing soil organic matter, *Organic Geochemistry*, *31*(7), 609-625.

711 Kujawinski, E. B., and M. D. Behn (2006), Automated analysis of electrospray ionization
712 Fourier transform ion cyclotron resonance mass spectra of natural organic matter, *Analytical*
713 *Chemistry*, *78*(13), 4363-4373.
714 Kuzyakov, Y. (2010), Priming effects: interactions between living and dead organic matter, *Soil*
715 *Biology and Biochemistry*, *42*(9), 1363-1371.
716 LaRowe, D. E., and P. Van Cappellen (2011), Degradation of natural organic matter: a
717 thermodynamic analysis, *Geochimica et Cosmochimica Acta*, *75*(8), 2030-2042.
718 Larson, J. H., P. C. Frost, M. A. Xenopoulos, C. J. Williams, A. M. Morales-Williams, J. M.
719 Vallazza, J. C. Nelson, and W. B. Richardson (2014), Relationships between land cover and
720 dissolved organic matter change along the river to lake transition, *Ecosystems*, *17*(8), 1413-1425.
721 Lehmann, J., and M. Kleber (2015), The contentious nature of soil organic matter, *Nature*,
722 *528*(7580), 60-68.
723 Lin, X., J. McKinley, C. T. Resch, R. Kaluzny, C. L. Lauber, J. Fredrickson, R. Knight, and A.
724 Konopka (2012), Spatial and temporal dynamics of the microbial community in the Hanford
725 unconfined aquifer, *The ISME Journal*, *6*(9), 1665-1676.
726 Lotspeich, F. B., and B. H. Reid (1980), Tri-tube freeze-core procedure for sampling stream
727 gravels, *The Progressive Fish-Culturist*, *42*(2), 96-99.
728 Mason, H., J. Begg, R. S. Maxwell, A. B. Kersting, and M. Zavarin (2016), A novel solid-state
729 NMR method for the investigation of trivalent lanthanide sorption on amorphous silica at low
730 surface loadings, *Environmental Science: Processes & Impacts*.
731 Minor, E. C., C. J. Steinbring, K. Longnecker, and E. B. Kujawinski (2012), Characterization of
732 dissolved organic matter in Lake Superior and its watershed using ultrahigh resolution mass
733 spectrometry, *Organic Geochemistry*, *43*, 1-11.
734 Moser, D. P., J. K. Fredrickson, D. R. Geist, E. V. Arntzen, A. D. Peacock, S.-M. W. Li, T.
735 Spadoni, and J. P. McKinley (2003), Biogeochemical processes and microbial characteristics
736 across groundwater-surface water boundaries of the Hanford Reach of the Columbia River,
737 *Environmental Science & Technology*, *37*(22), 5127-5134.
738 Peterson, R. E., and M. P. Connelly (2004), Water movement in the zone of interaction between
739 groundwater and the Columbia River, Hanford site, Washington, *Journal of Hydraulic Research*,
740 *42*(S1), 53-58.
741 Raffaele, S., A. Leger, and D. Roby (2009), Very long chain fatty acid and lipid signaling in the
742 response of plants to pathogens, *Plant signaling & behavior*, *4*(2), 94-99.
743 Regnier, P., P. Friedlingstein, P. Ciais, F. T. Mackenzie, N. Gruber, I. A. Janssens, G. G.
744 Laruelle, R. Lauerwald, S. Luyssaert, and A. J. Andersson (2013), Anthropogenic perturbation of
745 the carbon fluxes from land to ocean, *Nature geoscience*, *6*(8), 597-607.
746 Rood, K., and M. Church (1994), Modified freeze-core technique for sampling the permanently
747 wetted streambed, *North American Journal of Fisheries Management*, *14*(4), 852-861.
748 Rossel, P. E., C. Bienhold, A. Boetius, and T. Dittmar (2016), Dissolved organic matter in pore
749 water of Arctic Ocean sediments: Environmental influence on molecular composition, *Organic*
750 *Geochemistry*, *97*, 41-52.
751 Rothman, D. H., and D. C. Forney (2007), Physical model for the decay and preservation of
752 marine organic carbon, *Science*, *316*(5829), 1325-1328.
753 Schmidt, M. W., M. S. Torn, S. Abiven, T. Dittmar, G. Guggenberger, I. A. Janssens, M. Kleber,
754 I. Kögel-Knabner, J. Lehmann, and D. A. Manning (2011), Persistence of soil organic matter as
755 an ecosystem property, *Nature*, *478*(7367), 49-56.

Shepherd, T., and D. Wynne Griffiths (2006), The effects of stress on plant cuticular waxes, *New Phytologist*, *171*(3), 469-499.

Six, J., P. Callewaert, S. Lenders, S. De Gryze, S. Morris, E. Gregorich, E. Paul, and K. Paustian (2002), Measuring and understanding carbon storage in afforested soils by physical fractionation, *Soil science society of America journal*, *66*(6), 1981-1987.

Slater, L. D., D. Ntarlagiannis, F. D. Day‐Lewis, K. Mwakanyamale, R. J. Versteeg, A. Ward, C. Strickland, C. D. Johnson, and J. W. Lane (2010), Use of electrical imaging and distributed temperature sensing methods to characterize surface water–groundwater exchange regulating uranium transport at the Hanford 300 Area, Washington, *Water Resources Research*, *46*(10).

Smith, R. M., and S. S. Kaushal (2015), Carbon cycle of an urban watershed: exports, sources, and metabolism, *Biogeochemistry*, *126*(1-2), 173-195.

Stegen, J. C., J. K. Fredrickson, M. J. Wilkins, A. E. Konopka, W. C. Nelson, E. V. Arntzen, W. B. Chrisler, R. K. Chu, R. E. Danczak, and S. J. Fansler (2016), Groundwater-surface water mixing shifts ecological assembly processes and stimulates organic carbon turnover, *Nature Communications*, *7*.

Stegen, J. C., X. Lin, A. E. Konopka, and J. K. Fredrickson (2012), Stochastic and deterministic assembly processes in subsurface microbial communities, *The ISME Journal*, *6*(9), 1653-1664.

Tfaily, M. M., R. K. Chu, N. Tolić, K. M. Roscioli, C. R. Anderton, L. Pasa-Tolić, E. W. Robinson, and N. J. Hess (2015), Advanced solvent based methods for molecular characterization of soil organic matter by high-resolution mass spectrometry, *Analytical chemistry*, *87*(10), 5206-5215.

Tfaily, M. M., D. C. Podgorski, J. E. Corbett, J. P. Chanton, and W. T. Cooper (2011), Influence of acidification on the optical properties and molecular composition of dissolved organic matter, *Analytica chimica acta*, *706*(2), 261-267.

Tfaily, M. M., P. Reardon, R. K. Chu, N. Tolić, L. Pasa-Tolić, E. W. Robinson, and N. J. Hess (2017), Sequential extraction protocol for organic matter from soils and sediments using high resolution mass spectrometry and proton NMR, *Analytica Chimica Acta*.

Tholl, D. (2015), Biosynthesis and biological functions of terpenoids in plants, in *Biotechnology of Isoprenoids*, edited, pp. 63-106, Springer.

Todd-Brown, K., J. Randerson, W. Post, F. Hoffman, C. Tarnocai, E. Schuur, and S. Allison (2013), Causes of variation in soil carbon simulations from CMIP5 Earth system models and comparison with observations, *Biogeosciences*, *10*(3).

Trail, F., N. Mahanti, and J. Linz (1995), Molecular biology of aflatoxin biosynthesis, *Microbiology*, *141*(4), 755-765.

Tremblay, L. B., T. Dittmar, A. G. Marshall, W. J. Cooper, and W. T. Cooper (2007), Molecular characterization of dissolved organic matter in a North Brazilian mangrove porewater and mangrove-fringed estuaries by ultrahigh resolution Fourier transform-ion cyclotron resonance mass spectrometry and excitation/emission spectroscopy, *Marine chemistry*, *105*(1), 15-29.

Ward, C. P., and R. M. Cory (2015), Chemical composition of dissolved organic matter draining permafrost soils, *Geochimica et Cosmochimica Acta*, *167*, 63-79.

Wieder, W. R., G. B. Bonan, and S. D. Allison (2013), Global soil carbon projections are improved by modelling microbial processes, *Nature Climate Change*, *3*(10), 909-912.

Wieder, W. R., C. C. Cleveland, W. K. Smith, and K. Todd-Brown (2015), Future productivity and carbon storage limited by terrestrial nutrient availability, *Nature Geoscience*, *8*(6), 441-444.

Willaman, J. J., and B. G. Schubert (1961), *Alkaloid-bearing plants and their contained alkaloids*, Agricultural Research Service, US Department of Agriculture.

802 Zachara, J. M., P. E. Long, J. Bargar, J. A. Davis, P. Fox, J. K. Fredrickson, M. D. Freshley, A.
803 E. Konopka, C. Liu, and J. P. McKinley (2013), Persistence of uranium groundwater plumes:
804 Contrasting mechanisms at two DOE sites in the groundwater–river interaction zone, *Journal of*
805 *Contaminant Hydrology*, *147*, 45-72.
806 Zhang, L., S. Wang, Y. Xu, Q. Shi, H. Zhao, B. Jiang, and J. Yang (2016), Molecular
807 characterization of lake sediment WEON by Fourier transform ion cyclotron resonance mass
808 spectrometry and its environmental implications, *Water Research*, *106*, 196-203.
809
810

811 **Figure Captions and Table Legends.**

Figure 1

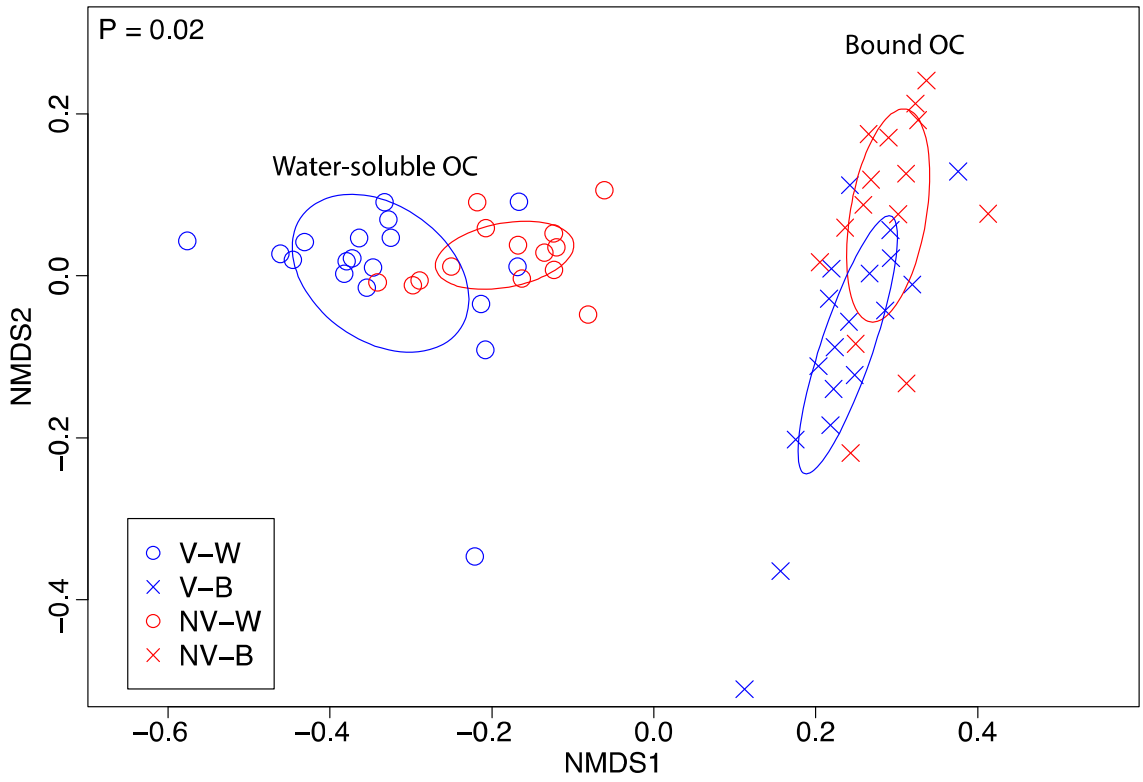

812

813 **Figure 1. NMDS visualization of dissimilarity in OC pool composition.** Water-soluble and
814 bound-OC pools are represented by open circles and x's, respectively. Samples associated with
815 riparian vegetation are blue, and those in areas without vegetation are red. The P-value reflects
816 differences among all groups, as assessed by PERMANOVA. Ellipses represent the standard
817 deviation of the average axis scores for each group, generated using the 'ordiellipse' function in
818 the 'vegan' package. Within each extraction, the composition of OC pools was significantly
819 different across vegetation states (both P = 0.001).

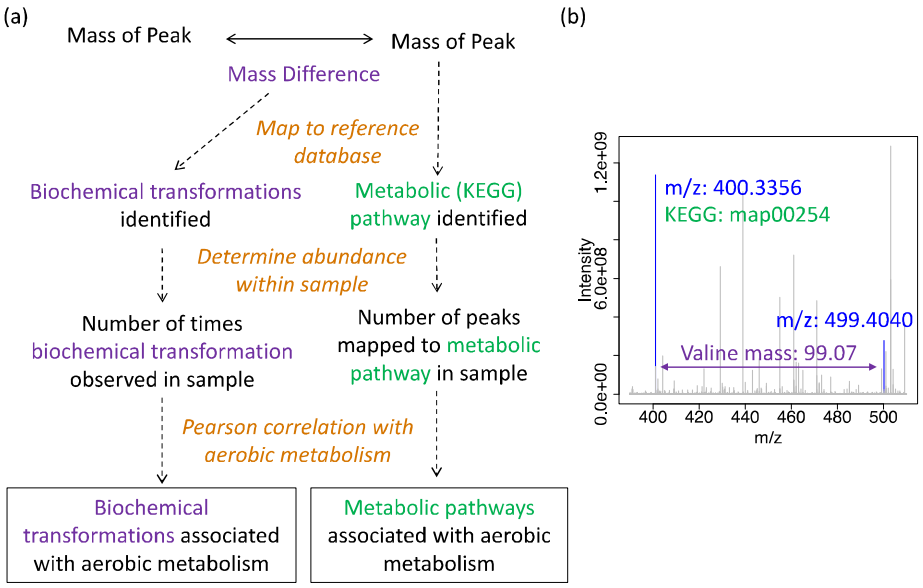

Figure 2. Methodology for inferring biochemical transformations and metabolic pathways. Panel (a) depicts our workflow for analyzing biochemical transformations and metabolic pathways. Biochemical OC transformations (purple) were identified by mapping mass differences in pairwise m/z peak comparisons to a set of 92 known masses transferred in common biochemical transformations (e.g., glucose, amines). Metabolic pathways (green) were identified by mapping all chemical formula assigned to m/z peaks to the KEGG database. Within each sample, the abundance of each biochemical transformation and the number of peaks mapping to each metabolic pathway were then correlated to aerobic metabolism to garner insights into OC oxidation processes. Panel (b) displays an example portion of our FT-ICR-MS spectra overlain with peak assignments (blue), a biochemical transformation (mass difference between peaks, denoted in purple), and a metabolic pathway (associated with the left-hand peak, denoted in green).

Figure 3

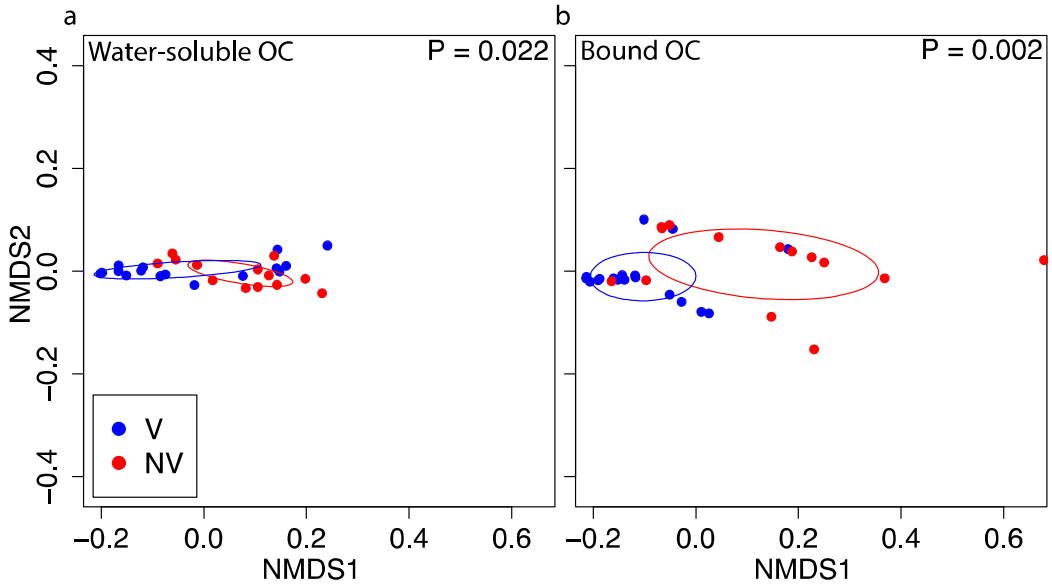

834
835 **Figure 3. NMDS visualization of biochemical transformation partitioning among vegetation**
836 **states.** Biochemical transformations that were correlated to aerobic metabolism were
837 significantly different among vegetation states in both the (a) water-soluble and (b) bound-OC
838 pools. V and NV are denoted in blue and red, respectively, and significance values are derived
839 from PERMANOVA. Ellipses represent the standard deviation of the average axis scores for
840 each group, generated using the 'ordiellipse' function in the 'vegan' package.
841
842

Figure 4

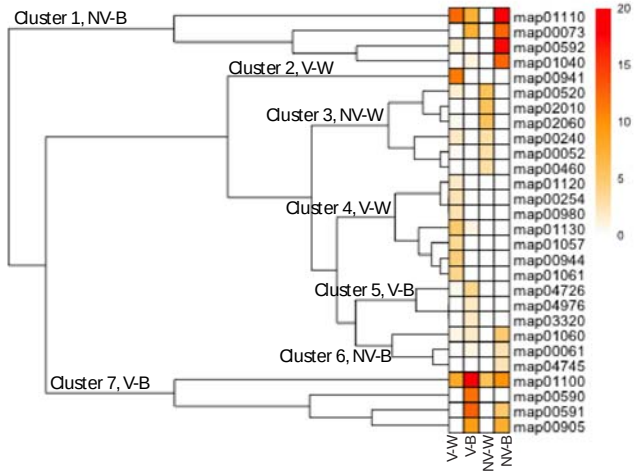

	Pathway	Pathway Description
	map01110	Biosynthesis of secondary metabolites
Cluster 1	map00073	Cutin, suberine and wax biosynthesis
NV-B	map00592	alpha-Linolenic acid metabolism
	map01040	Biosynthesis of unsaturated fatty acids
Cluster 2	map00941	Flavonoid biosynthesis
V-W		
	map00520	Amino sugar and nucleotide sugar metabolism
	map02010	ABC transporters
Cluster 3	map02060	Phosphotransferase system (PTS)
NV-W	map00240	Pyrimidine metabolism
	map00052	Galactose metabolism
	map00460	Cyanoamino acid metabolism
	map01120	Microbial metabolism in diverse environments
	map00254	Aflatoxin biosynthesis
Cluster 4	map00980	Metabolism of xenobiotics by cytochrome P450
V-W	map01130	Biosynthesis of antibiotics
	map01057	Biosynthesis of type II polyketide products
	map00944	Flavone and flavonol biosynthesis
	map01061	Biosynthesis of phenylpropanoids
	map04726	Serotonergic synapse
Cluster 5	map04976	Bile secretion
V-B	map03320	PPAR signaling pathway
	map01060	Biosynthesis of plant secondary metabolites
Cluster 6	map00061	Fatty acid biosynthesis
NV-B	map04745	Phototransduction - fly
	map01100	Metabolic pathways
Cluster 7	map00590	Arachidonic acid metabolism
V-B	map00591	Linoleic acid metabolism
	map00905	Brassinosteroid biosynthesis

Figure 4. KEGG pathways associated with aerobic metabolism. A hierarchical clustering heatmap shows KEGG pathways positively associated with aerobic metabolism. Colors move from white to red from a scale of 0% to 20%, showing percent relative abundance of each pathway in each group. Pathways are described and divided by cluster and listed in the legend. V-W, V-B, NV-W, and NV-B are placed on branches that yield clusters with which they are predominantly associated.

Figure 5

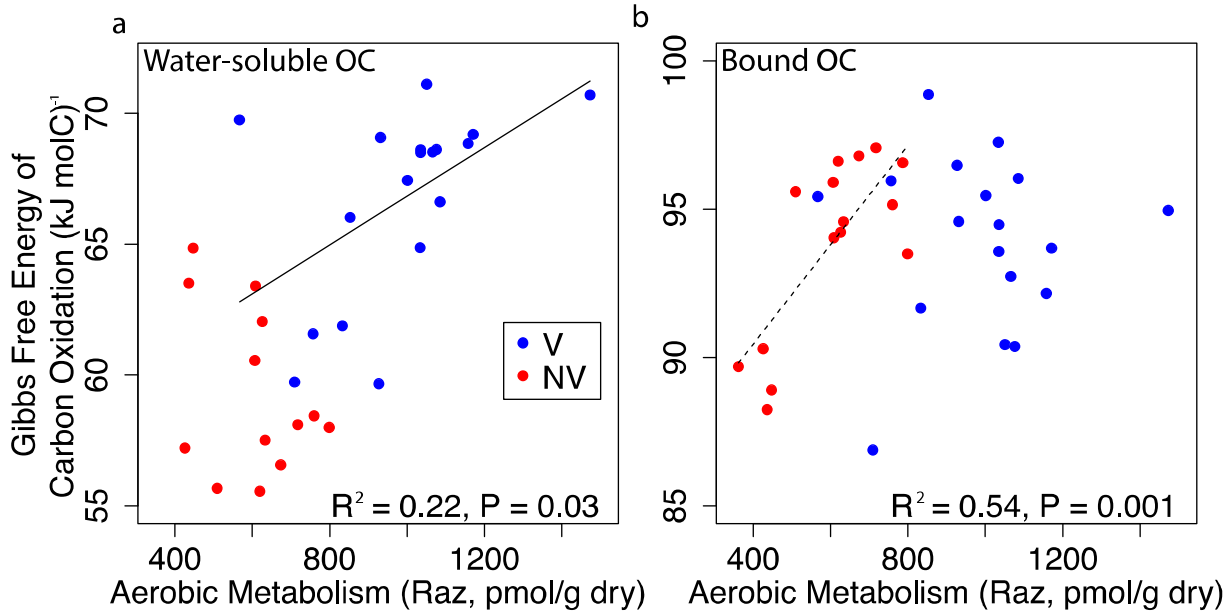

Figure 5. Correlations between Gibbs free energy of carbon oxidation (ΔG^{o}_{Cox}) and aerobic metabolism. (a) and (b) display linear regressions relating ΔG^{o}_{Cox} to aerobic metabolism in water-soluble and bound-OC pools, respectively. Aerobic metabolism is expressed as pmoles of resazurin reduced to resorufin per gram dry weight over a 48hr incubation period (Raz, see Supplemental Information). V and NV are denoted in blue and red. Solid lines show significant relationship at V; dashed lines show significant relationship at NV.

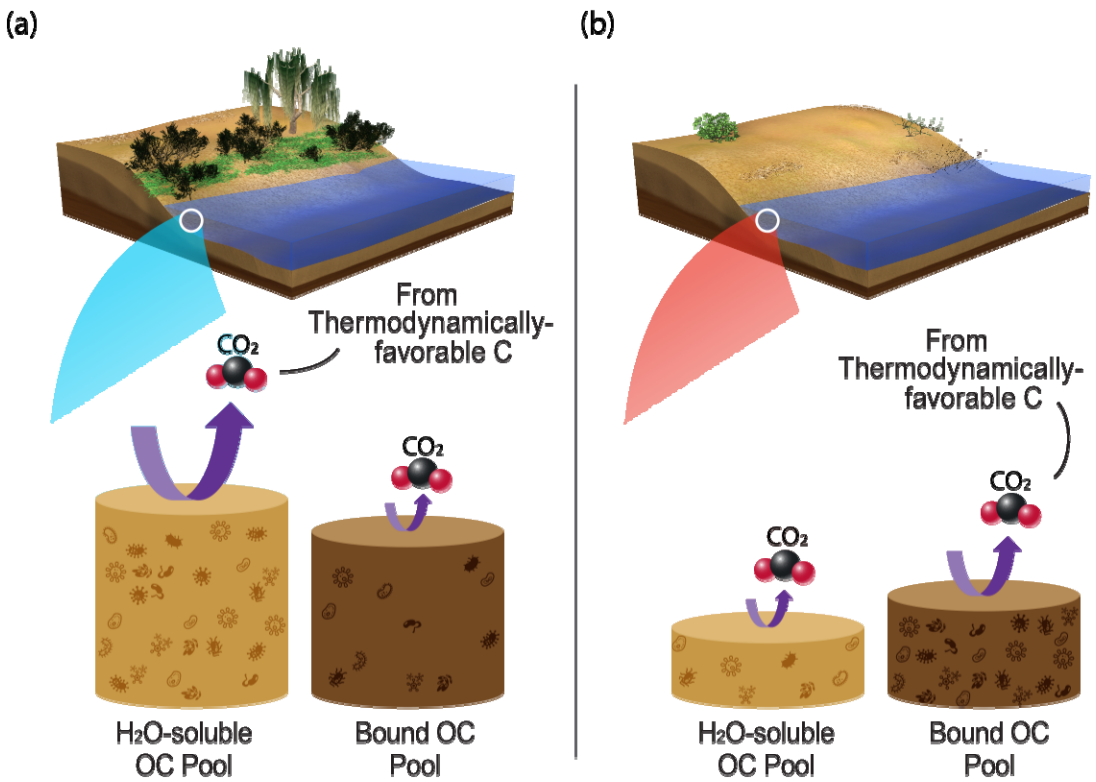

Figure 6. Conceptualization of relationship between riparian vegetation and OC oxidation. We propose a conceptualization of OC oxidation at terrestrial-aquatic interfaces whereby (a) more riparian vegetation results in greater terrestrial C deposition and larger water-soluble and bound-OC pools. However, water-soluble OC is preferentially oxidized, which protects the bound-OC pool. Conversely, (b) areas deplete in riparian vegetation experience lower inputs to water-soluble OC pools and show lower rates of OC oxidation. This results in smaller OC pools (water-soluble and bound) and microbial adaptation for oxidation of the bound-OC pool. In both cases, the most thermodynamically favorable portions of the OC pool being metabolized are preferentially oxidized. Height of the cylinders denotes pool sizes, and arrow thickness denotes flux magnitude.

873 **Table 1. Acronyms and abbreviations used in this paper.**

Abbreviation/Acronym	Description
V	Transect with dense riparian vegetation (i.e., 'vegetated')
NV	Transect with sparse riparian vegetation (i.e., 'not vegetated')
V-W	Transect V, water extraction (water-soluble OC)
V-B	Transect V, chloroform extraction (bound-OC)
NV-W	Transect NV, water extraction (water-soluble OC)
NV-B	Transect NV, chloroform extraction (bound-OC)
H_2O	Water
$CHCl_3$	Chloroform
C	Carbon
OC	Organic carbon
FT-ICR-MS	Fourier transform ion cyclotron resonance mass spectrometry
KEGG	Kyoto Encyclopedia of Genes and Genomes
ΔG^{o}_{Cox}	Gibbs free energy of C oxidation

874

875 **Table 2. Biochemical transformations correlated with aerobic metabolism in each OC pool**

876 **and vegetation state.**

	Pearson's r
V-W	
biotinyl_(-H)_C10H15N2O3S	0.74
uridine_5_diphosphate_(-H2O)_C9H12N2O11P2	0.67
cytosine_(-H)_C4H4N3O	0.65
uridine_5_monophosphate_(-H2O)_C9H11N2O8P	0.65
guanine_(-H)_C5H4N5O	0.61
guanosine_(-H2O)_C10H11N5O4	0.59
adenine_(-H)_C5H4N5	0.59
glutathione_(-H2O)_C10H15N3O5S	0.57
uracil_(-H)_C4H3N2O2	0.56
glucose_C6H12O6	0.53
C6H10O6	0.53
Aspartic_Acid_C4H5NO3	0.52
GlucuronicAcid(-H2O)	0.52
Lysine_C6H12N2O	0.51
D-Ribose(-H2O)(ribosylation)	0.50
secondaryamine	0.50
Alanine_C3H5NO	0.50
C6H10O5	0.49
monosaccharide(-H2O)	0.49
Threonine_C4H7NO2	0.49
Glutamic_Acid_C5H7NO3	0.48
pentose_C5H8O4	0.47
acetotacetate_(-H2O)_C4H4O2	0.47
Glutamine_C5H8N2O2	0.47
pyridoxal_phosphate_(-H2O)_C8H8NO5P	0.47
V-B	
isoprene_addition_(-H)_C5H7	0.61
phosphate	0.56
primaryamine	0.55
GlucuronicAcid(-H2O)	0.53
glyoxylate_(-H2O)_C2O2	0.53
malonyl_group_(-H2O)_C3H2O3	0.52
D-Ribose(-H2O)(ribosylation)	0.49
pyrophosphate	0.49
acetotacetate_(-H2O)_C4H4O2	0.49
hydrogenation_dehydrogenation_H2	0.47

877

NV-W	
NONE	NA
NV-B	
Adenosine_5_monophosphate_(-H2O)_C10H12N5O6P	0.92
adenylate_(-H2O)_C10H12N5O6P	0.92
pyridoxal_phosphate_(-H2O)_C8H8NO5P	0.73
acetylation_(-H2O)_C2H2O	0.70
ketol group (-H2O)	0.70
Isoleucine_C6H11NO	0.69
Leucine_C6H11NO	0.69
ethyl addition_(-H2O)_C2H4	0.69
Threonine_C4H7NO2	0.69
Valine_C5H9NO	0.68
Carboxylation_CO2	0.68
Glycine_C2H3NO	0.67
Formic Acid_(-H2O)_CO	0.67
Serine_C3H5NO2	0.67
hydroxylation_(-H)_O	0.67
palmitoylation_(-H2O)_C16H30O	0.67
pentose_C5H8O4	0.66
secondary amine	0.66
condensation/dehydration_H2O	0.66
C2H2_C2H2	0.66
erythose (-H2O)	0.66
CH4_O	0.65
methanol (-H2O)	0.65
glyoxylate_(-H2O)_C2O2	0.65
NH_CH2	0.64
Alanine_C3H5NO	0.63
acetotacetate_(-H2O)_C4H4O2	0.63
Proline_C5H7NO	0.62
hydrogenation_dehydrogenation_H2	0.61
Histidine_C6H7N3O	0.60
malonyl_group_(-H2O)_C3H2O3	0.59
Cysteine_C3H5NOS	0.58
glcnac_C8H13N1O5	0.57
Methionine_C5H9NOS	0.57
Arginine_C6H12N4O	0.56
Aspartic_Acid_C4H5NO3	0.56

D-Ribose (-H2O) (ribosylation)	0.55